JOURNAL OF CATALYSIS 135, 125–134 (1992)

Structural and Acidic Characterization of Niobia Aerogels

S. M. MAURER AND E. I. KO[1]

Department of Chemical Engineering, Carnegie Mellon University, Pittsburgh, Pennsylvania 15213

Received August 20, 1991; revised November 4, 1991

A niobia (Nb_2O_5) gel was prepared by the hydrolysis and condensation of niobium pentaethoxide and subsequently dried by supercritical extraction with carbon dioxide to produce an aerogel. The structural and acidic properties of this aerogel heat-treated at different temperatures were characterized by surface area measurements, X-ray diffraction, Raman spectroscopy, *n*-butylamine titration, pyridine adsorption, and 1-butene isomerization. These results were then compared to those of a niobia xerogel, a precipitated niobia, and a commercial niobic acid. The synthetic route to produce the aerogel was found to stabilize a porous network consisting of NbO_6 octahedra with Nb=O bonds which gave rise to strong Lewis acid sites. Steady-state activity and selectivity data of 1-butene isomerization suggested that all niobia samples possessed comparable Brønsted acidity.

INTRODUCTION

In recent years sol–gel processing has received a lot of attention in the preparation of glasses and ceramics (*1*). One particularly interesting class of materials is aerogels, which are obtained by removing the solvent from wet gels with supercritical extraction. The technique of preparing aerogels was first developed in the 1930s by Kistler, who used alcohol as an extracting solvent in a batch process (*2, 3*). Over the years the technology has evolved to the point that it is safer and easier to run a semi-continuous process with supercritical carbon dioxide (*4*).

The purpose of using supercritical extraction for solvent removal is to eliminate the liquid–vapor interface inside the capillaries of a porous gel. By avoiding the interfacial tension which often causes the collapse of the porous texture during conventional drying, it becomes possible to obtain aerogels which are low density, extremely porous, and have large surface areas (*5*). These properties make aerogels desirable as catalysts or catalyst supports, a potential application which was also recognized by Kistler in his pioneering work (*6*). But this area of research remained largely unexplored until Teichner and his co-workers demonstrated the successful synthesis of a large number of single and mixed oxides as aerogels (*7, 8*). Since then there have been many reports on the catalytic properties of aerogels as recently reviewed by Pajonk (*9*). Still the literature on the sol–gel synthesis of catalytic materials, especially as aerogels, is not as extensive as that on the synthesis of glasses and ceramics (*1*). Although one can certainly learn from the literature on glasses and ceramics, the different end-use properties of catalytic materials (for example, low rather than high density is desirable) often involve using different synthetic parameters. There is also a need to further characterize the chemical properties of aerogels which are of catalytic interest.

We have for many years been interested in the catalytic behavior of niobia (Nb_2O_5) and, in an attempt to maximize its surface area, undertaken a study to prepare Nb_2O_5 as aerogels. In an earlier report (*10*) we showed that Nb_2O_5 prepared as aerogels indeed have a significantly larger surface area than samples prepared by conventional methods such as precipitation. In this paper

[1] To whom correspondence should be addressed.

0021-9517/92 $3.00

TABLE 1

Experimental Conditions for the Synthesis of Niobia Aerogel and Xerogel

Step	Conditions
Dissolution	1. Dissolve 25 mmol of niobium ethoxide in 25 ml of *s*-butyl alcohol. 2. Add 250 mmol of doubly deionized water and 20 mmol of nitric acid to a second 25 ml of *s*-butyl alcohol. 3. Stir both solutions for 10 min to homogenize.
Hydrolysis/Condensation	1. Mix both solutions in a beaker under constant agitation with a magnetic stir bar. 2. Allow to hydrolyze and polymerize; a gel forms in about 10 s.
Aging	1. Allow the gel to age at room temperature for about 1 h.
Solvent removal	1. Extract using supercritical CO_2 at 343 K, 3000 psi, and 0.05 SCFM for 2 to 3 h (for aerogel), or 2. Heat in a vacuum oven at 383 K for 3 h (for xerogel).
Calcination	1. Heat in flowing nitrogen (300 cc/min) from room temperature to 673 K at 10 K/min and then at 673 K for 2 h. 2. Heat in flowing oxygen (300 cc/min) from 673 K to 773 K at 10 K/min and then at 773 K for 2 h.

we present a more detailed characterization of these aerogels. Specifically, we have studied their structural and acidic properties as a function of heat treatment and compared these samples with niobic acid, a hydrated niobia which has been found active in many acid-catalyzed reactions (*11*).

METHODS

Sample Preparation

Table 1 summarizes the steps and conditions for the preparation of niobia aerogels and xerogels. Niobia gels were prepared by dissolving 25 mmol of the precursor, niobium (V) ethoxide [$Nb(OC_2H_5)_5$, Alfa], in 25 ml of *s*-butyl alcohol (99+% anhydrous, Aldrich). This solution was quickly added to a well-mixed solution containing 25 ml of *s*-butyl alcohol, 250 mmol of doubly deionized water, and 20 mmol of nitric acid (70%, Fisher). Under these conditions the resulting solution turned into a clear gel in about 10 s. The gel was then extracted in a standard autoclave (Autoclave Engineers, Model 08U-06-60FS) with supercritical CO_2 (Airco) at ca. 343 K and 2.07×10^7 Pa (3000 psi). With a CO_2 flow rate of 2.36×10^{-5} m^3/s (0.05 SCFM), a typical extraction lasted for 2–3 h for the complete removal of solvent. Subsequent to extraction, the sample was heated in a tube furnace in flowing nitrogen at 673 K for 2 h and then in flowing oxygen at 773 K for 2 h, which was the standard calcination procedure in this study. The Nb_2O_5 aerogel thus obtained is denoted as A-Nb_2O_5.

Two other Nb_2O_5 samples were prepared for comparison. A precipitated sample, denoted as P-Nb_2O_5, was made by adding ammonium hydroxide dropwise to a methanolic solution of niobium ethoxide. The precipitate was washed and filtered and then dried in a vacuum oven at 383 K for 3 h. A xerogel, denoted as X-Nb_2O_5, was made by bypassing the supercritical extraction step in the synthesis of the aerogel. Instead, a Nb_2O_5 gel was dried in a vacuum oven at 383 K for 3 h to produce the xerogel.

The niobic acid (Niobia-HY®-340) used in this study was a hydrated niobium pentoxide manufactured by CBMM (Companhia Brasileira de Matalurgia e Mineracao).

Physical Characterization

BET surface areas of the samples were measured with the single-point method on a

commercial Quantasorb unit (Quantachrome Corp.). These values were checked against those obtained with the multi-point method on selected samples, and the agreement was within a few percent. Analyses of pore size distribution and pore volume were done by Porous Materials, Inc. (PMI), using nitrogen adsorption data. The Kelvin equation was used to calculate the pore radius as a function of relative pressure and the total pore volume was determined from the amount adsorbed at a relative pressure close to unity.

Powder X-ray diffraction patterns were obtained with a Rigaku D/Max diffractometer using a Mo source. A JEOL CAM-SCAN scanning electron microscope (SEM) was used to study the morphology of the samples. Raman spectra were taken at the Zettlemoyer Center for Surface Studies at Lehigh University. Details of the Raman spectrometer and experimental procedure can be found elsewhere (*12*).

Acidity Measurements

The acidic properties of the samples were characterized by four techniques which have been in use in our laboratory (*13, 14*). The acid site distribution was determined by titrating a sample, which had been pretreated in a vacuum oven at 373 K for 1 h just prior to titration, in benzene with *n*-butylamine using a procedure similar to the Benesi method (*15*). All titrations were done using a digital pipette of 0.01-ml resolution with the sample vigorously stirred by a micromagnetic bar. Even though the titration technique has intrinsic limitations, we took precautions to ensure that the results are reproducible and that they can be meaningfully compared on a relative basis (*13*).

The adsorption of pyridine was used to (i) determine the heat of adsorption by using a thermogravimetric procedure similar to that of Deeba and Hall (*16*), and (ii) to distinguish between Lewis and Brønsted acid sites. Thermogravimetric measurements were made with a Cahn 113 microbalance. Infrared spectra were obtained with an IBM 98 FTIR spectrometer.

1-Butene isomerization was carried out in a continuous-flow, stainless-steel microreactor operated in a differential mode at 423 K and atmospheric pressure. In a typical run a 100–200 mg sample was conditioned in the reactor in flowing He (3 l/h) at room temperature for 2–3 h and subsequently at 473 K for 1 h. The reactor temperature was then adjusted to 423 K and 0.3 l/h of 1-butene was mixed with 5.7 l/h of He to give a reaction mixture of 5 mol% 1-butene and 95 mol% He. After the reaction mixture was fed through the top of the reactor, the outlet gas mixture was sampled and analyzed every 12 min by a gas chromatograph (Gow-Mac, Series 550P) until steady-state activity was reached. A stainless steel column containing 0.19 wt% picric acid on 80/100 mesh Carbopack C packing (Supelco, Inc.) was used to separate 1-butene, *cis*- and *trans*-2-butene.

RESULTS

Physical Properties

Table 2 summarizes the BET surface area and pore volume of the samples after the standard calcination. Whereas X-Nb_2O_5, P-Nb_2O_5, and niobic acid have similar physical characteristics, A-Nb_2O_5 has a surface area which is twice as high, a pore volume which is almost an order of magnitude higher, and a pore size distribution which is significantly different from that of X-Nb_2O_5 (see Fig. 1). Figure 2 also shows

TABLE 2

Physical Characteristics of Samples after Calcination at 773 K for 2h

Sample	BET surface area (m^2/g)	Pore volume (cm^3/g)
A-Nb_2O_5	190	1.280
X-Nb_2O_5	100	0.184
P-Nb_2O_5	85	0.153
Niobic acid	100	0.129

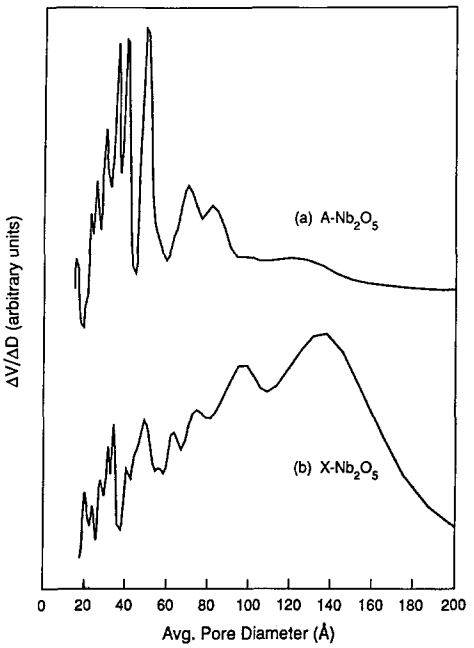

FIG. 1. Pore size distribution data of (a) A-Nb_2O_5 and (b) X-Nb_2O_5.

the morphology of this sample to be different from that of the other two Nb_2O_5 samples. Furthermore, A-Nb_2O_5 is the only sample which remains X-ray amorphous after the standard calcination (see Table 3).

Tables 3 and 4 show the effect of heat treatment on the structure and surface area of these samples. A-Nb_2O_5 crystallizes into the TT-form (*17*) after heating at 873 K for 2 h and along with it, has a significant reduction in surface area. The loss in surface area continues with more severe thermal treatments and the corresponding change in Nb_2O_5 modification (TT → T → M) agrees with what has been previously reported (*17, 18*). The surface areas after the (1273, —) treatment are so low that, with the uncertainty of the single-point BET method, they should be viewed as relative rather than absolute values.

Figure 3 shows the Laser Raman spectra for A-Nb_2O_5 heat-treated at different temperatures to produce the amorphous, TT-, and T-forms. The peak at ca. 700 cm^{-1}, which has been assigned to a distorted octahedral NbO_6 structure (*12*), is present in all three samples. On the other hand, only the amorphous A-Nb_2O_5 has a peak in the 850-1000 cm^{-1} region, which has been assigned to a highly distorted octahedral NbO_6 structure containing a Nb=O bond (*12*). *In-situ* Raman data further show that heating the sample to desorb water revealed two Raman bands at 930 and 990 cm^{-1} (see Fig. 4) which are characteristic of two different highly distorted Nb=O species (*12*). These changes in spectral features are reversible upon rehydration, suggesting the Nb=O species to be a surface functionality.

Chemical Properties

Figure 5 shows the acidic site distribution determined by *n*-butylamine titration for

TABLE 3

Phases of Nb_2O_5 Identified by X-ray Diffraction as a Function of Heat Treatment[a]

Heat treatment (temperature in K, time in h)	A-Nb_2O_5	X-Nb_2O_5	P-Nb_2O_5	Niobic acid
(773, 2)	A[b]	TT	TT	TT_{pc}[b]
(873, 2)	TT	TT	TT	TT
(1073, 2)	T	T	T	T
(1273, —)[c]	M	M	T + M	T + M

[a] The notation of Shafer *et al.* (*17*) is used to describe the modifications of Nb_2O_5: TT and T, low-temperature forms; and M, medium-temperature form.

[b] A = amorphous, pc = poorly crystalline.

[c] (1273, —) means the sample was ramped to 1273 K at 10 K/min without being held at that temperature.

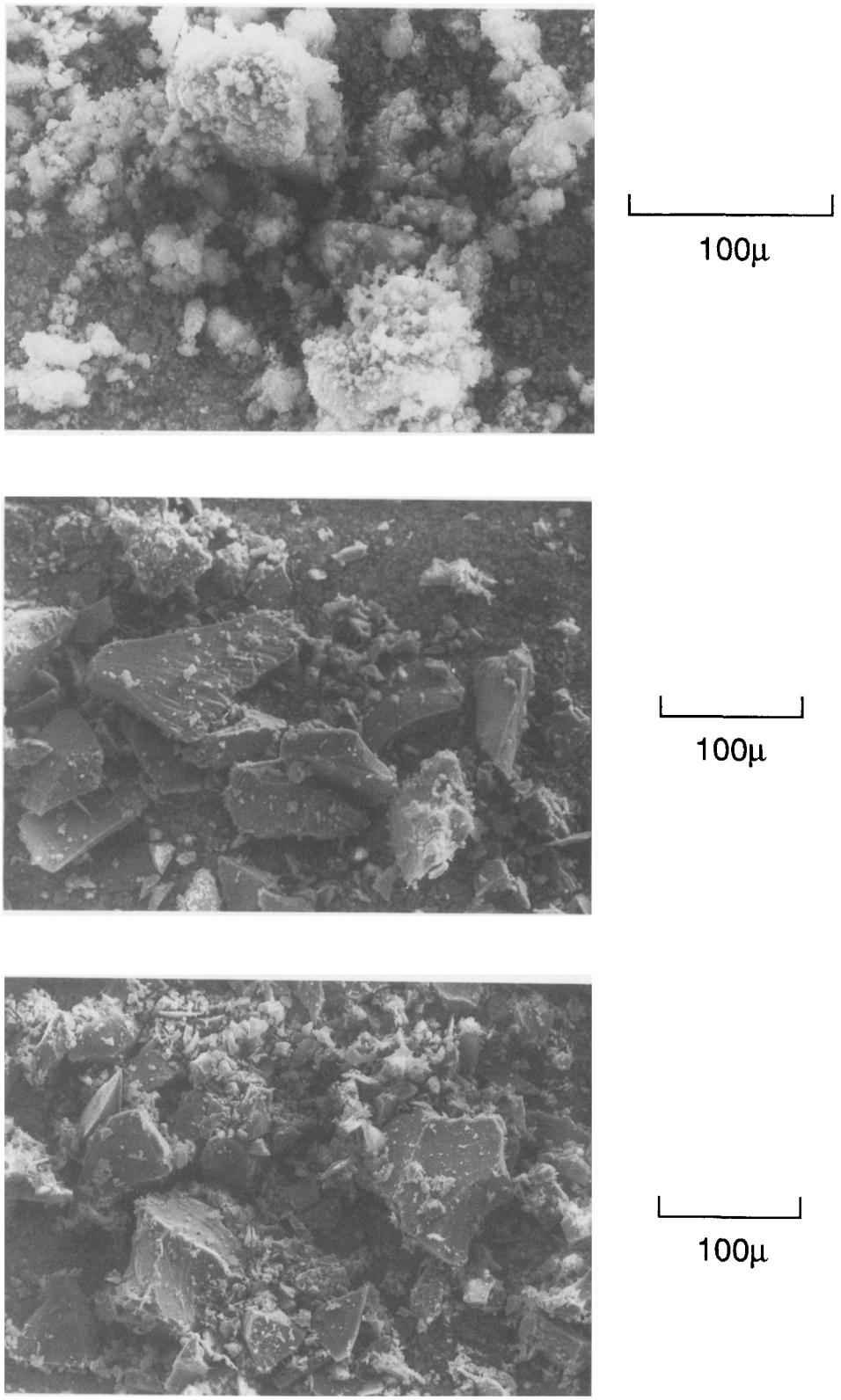

FIG. 2. SEM micrographs of A-Nb_2O_5 (top), P-Nb_2O_5 (middle), and X-Nb_2O_5 (bottom) heat treated at 773 K for 2 h.

TABLE 4

Surface Area as a Function of Heat Treatment

Heat treatment (temperature in K, time in h)	Surface Area (m^2/g)			
	A-Nb_2O_5	X-Nb_2O_5	P-Nb_2O_5	Niobic acid
(773, 2)	190	100	85	100
(873, 2)	60	35	30	25
(1073, 2)	5	4	4	3.5
(1273, —)[a]	1	1	1	0.5

[a] See Table 3.

three Nb_2O_5 samples after the standard calcination. It is clear that A-Nb_2O_5 has more acid sites at all pK_a ranges studied than P-Nb_2O_5 and X-Nb_2O_5 either on a per-mass or per-surface-area basis. Included in the same figure are the data for niobic acid, a commercial sample which has been found active for many acid-catalyzed reactions (*11*). On the basis of acid site distribution, then, A-Nb_2O_5 compares favorably with niobic acid, especially in view of the fact that the latter was not calcined to as high a temperature. In fact, data for niobic acid correspond to an uncalcined sample, since it is well known that the acid amount of niobic acid decreases with increasing calcination

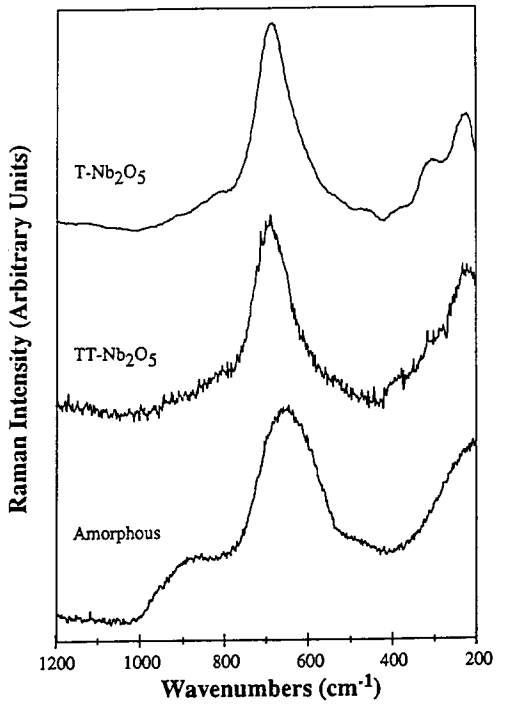

FIG. 3. Laser Raman spectra of A-Nb_2O_5 heat treated at (773, 2) (bottom), (873, 2) (middle), and (1073, 2) (top). The X-ray diffraction result of each sample (see Table 3) is also indicated.

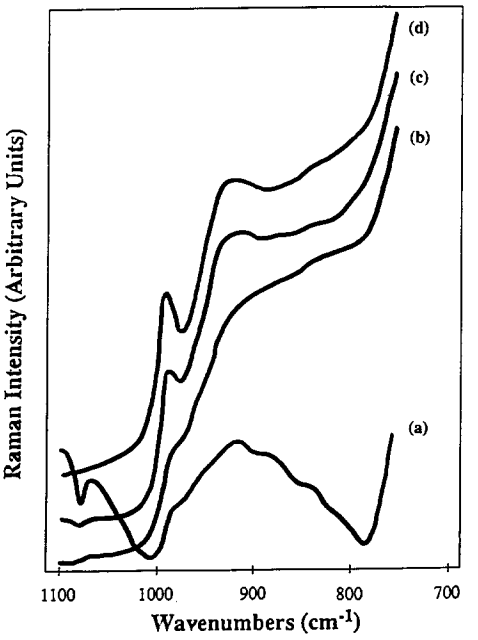

FIG. 4. *In-situ* laser Raman spectra of A-Nb_2O_5: (a) hydrated sample, (b) evacuated at 373 K for 1 h, (c) evacuated at 473 K for 1 h, and (d) evacuated at 773 K for 1 h.

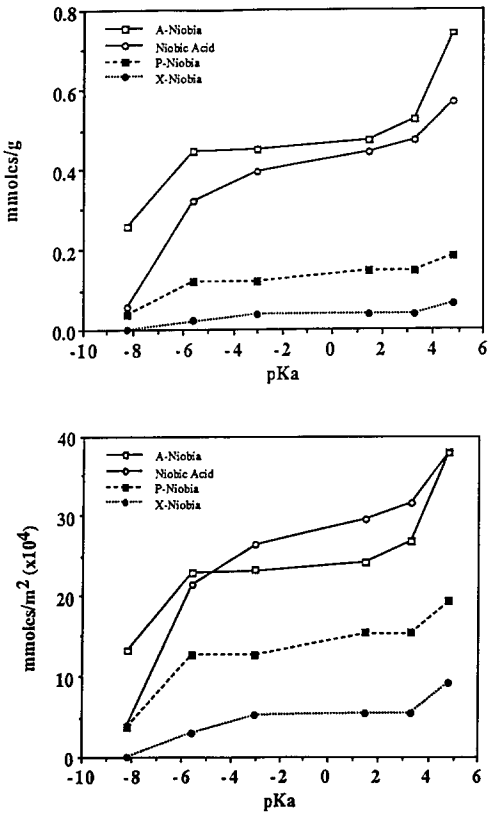

FIG. 5. Comparison of acid site distributions of niobia samples as determined by *n*-butylamine titration. Acid amounts are reported in terms of mass of the sample (top panel) and surface area of the sample (bottom panel).

temperature (*19*). Compared at the same calcination temperature of 773 K, A-Nb_2O_5 has more acid amounts at all pK_a ranges than niobic acid (*20*).

Figure 6 shows the effect of heat treatment on the acid site distribution of A-Nb_2O_5. The most noticeable difference is in the strongest acid sites at pK_a = −8.2, which are totally gone with the crystallization of TT-Nb_2O_5 at 873 K. Since P- and X-Nb_2O_5 in the TT-form also have little to no acid sites at this pK_a (see Fig. 5), these data suggest a strong acidity–structure relationship in the Nb_2O_5 samples. We return to this point in the Discussion.

The adsorption of pyridine provided additional information on the nature of acid sites in A-Nb_2O_5. After the standard calcination, the heat of adsorption for pyridine is higher on A-Nb_2O_5 than on P-Nb_2O_5 (see Fig. 7), consistent with the presence of stronger acid sites in the former sample. FTIR data (see Fig. 8) further showed the presence of both Lewis and Brønsted acid sites in A-Nb_2O_5, as there are bands at ca. 1550 cm^{-1} arising from pyridinium ions and at ca. 1450 cm^{-1} arising from coordinately bound pyridine (*21*). Following the method of Basila and Kantner (*22*), we calculated the ratio of Lewis to Brønsted acid sites to be 3.3, 7.7, and 25 after evacuation at 373, 473, and 573 K, respectively. In other words, pyridine desorbed preferentially from Brønsted acid sites with increasing evacuation temperature, which is demon-

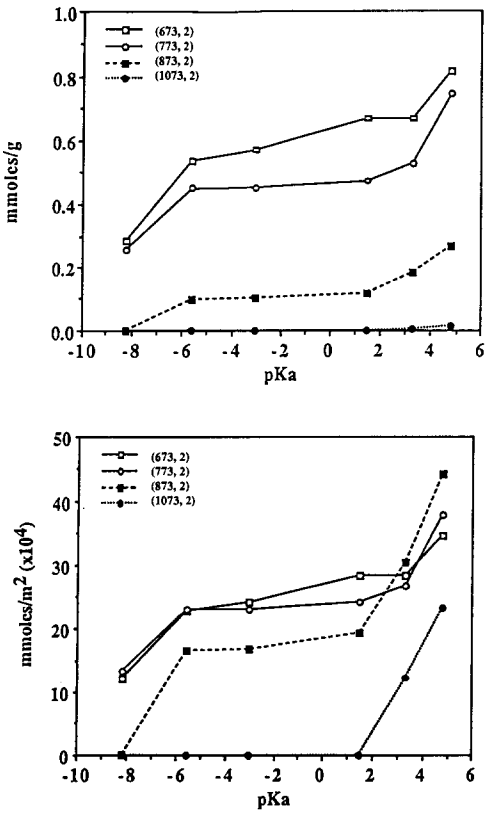

FIG. 6. Effect of heat treatment (temperature in K, time in h) on the acid site distribution of A-Nb_2O_5: (top panel) per mass of the sample, and (bottom panel) per surface area of the sample.

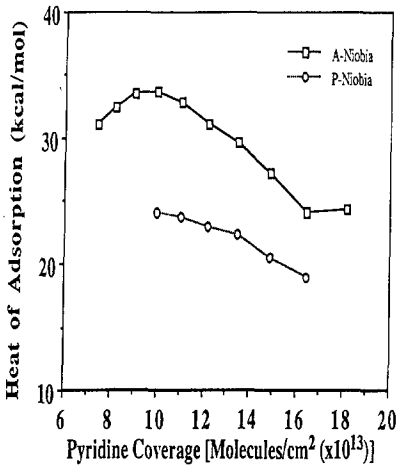

FIG. 7. Heat of adsorption as a function of pyridine coverage for A-Nb_2O_5 and P-Nb_2O_5.

strated in Fig. 8 in the relative intensity of the 1550 and 1450 cm^{-1} peaks.

Although A-Nb_2O_5, P-Nb_2O_5, and X-Nb_2O_5 have different acid site distributions, they have comparable steady-state activities, reported on a per-surface-area basis, for the isomerization of 1-butene (see

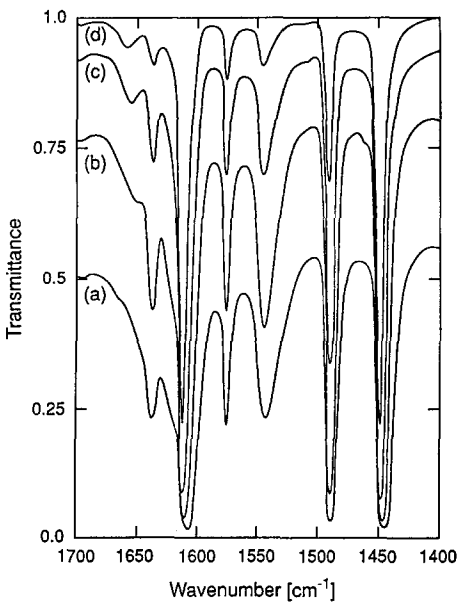

FIG. 8. FTIR spectra of pyridine adsorbed on A-Nb_2O_5 after evacuation at (a) 298 K, (b) 373 K, (c) 473 K, and (d) 573 K.

TABLE 5

Kinetic Data of 1-Butene Isomerization

Sample	Activity at 423 K (mol/h/m^2, $\times 10^{-4}$)	*cis*/*trans*-2-butene
A-Nb_2O_5[a]	0.71	1.6
P-Nb_2O_5[a]	0.71	1.4
X-Nb_2O_5[a]	0.53	0.7
Niobic acid[b]	0.74	0.7
A-Nb_2O_5 (873, 2)[c]	0.53	1.3
A-Nb_2O_5 (1073, 2)[d]	0.73	1.1

[a] Calcined at 773 K for 2 h.
[b] Not calcined.
[c] Calcined at 873 K for 2 h.
[d] Calcined at 1073 K for 2 h.

Table 5). These observations are not inconsistent with the data in Fig. 5, since 1-butene isomerization is catalyzed by Brønsted acid sites (*23, 24*), whereas *n*-butylamine titration measures both Lewis and Brønsted acid sites. As shown in Table 5, the selectivities of these samples, reported as the ratio of *cis*- to *trans*-2-butene, range from 0.7–1.6 and are consistent with the formation of a 2-butyl carbonium ion intermediate on Brønsted acid sites (*24*). As a further evidence that these samples have comparable Brønsted acidity for isomerization, results in Table 5 showed that A-Nb_2O_5 heat-treated at 873 and 1073 K maintain the same activity (per surface area) and selectivity, even though the same samples show a significant decline in total acidity as determined by *n*-butylamine titration (see Fig. 6).

DISCUSSION

The chemistry of the sol–gel process has been extensively studied for silica but much less so for transition metal oxides (*1, 25*). Although the synthesis of niobia gels has been previously reported (*26, 27*), to our knowledge this work represents the first study of niobia aerogels with catalytic applications in mind.

In an EXAFS study of the hydrolysis of niobium pentaethoxide, Vandenborre *et al.*

(*27*) reported that Nb_2O_5 gels contain corner sharing NbO_6 octahedra and exhibit a rather open structure. An open structure for the gel network would be consistent with the high surface area and large pore volume of our Nb_2O_5 aerogel which was synthesized via a similar procedure. The important point, though, is the integrity of the gel network can only be preserved through removal of the solvent by supercritical extraction (often referred to as hypercritical drying). This procedure eliminates the liquid–vapor interface in the capillaries of the gel during conventional drying which acts to collapse the pores (*5, 8*). This point is most vividly demonstrated by the very different physical characteristics (surface area, pore volume, and morphology) of A-Nb_2O_5 and X-Nb_2O_5, as the two samples came from the same gel and differed only in the way they were dried. Results in Fig. 1 clearly demonstrate that even though both of these samples have a wide pore size distribution, A-Nb_2O_5 has relatively more pores with diameter in the 2–6 nm region than X-Nb_2O_5. The similarity between X-Nb_2O_5 and P-Nb_2O_5 further suggests that unless a gel is dried properly, there is no advantage in its surface area over that of a precipitated sample.

A-Nb_2O_5 aerogel should thus be viewed as a stable, porous material. However, it must be emphasized that the synthesis does not produce a new thermodynamically stable phase, but simply stabilizes a porous network by lowering the mobility necessary for the atoms to sinter and crystallize. In other words, it is a kinetic constraint which maintains the high surface area of A-Nb_2O_5 and keeps it amorphous after calcination at 773 K for 2 h. When the kinetic constraint is overcome by more severe heat treatments, A-Nb_2O_5 crystallizes and loses surface area in the same way as conventionally prepared samples (see Tables 3 and 4).

Although high surface area is by itself a desirable property in a catalytic material, the stabilization of A-Nb_2O_5 actually leads to another interesting feature. Raman data showed the presence of NbO_6 octahedra, which is consistent with the observation of Vandenborre *et al.* (*27*), and more importantly, with the presence of Nb=O bonds. We believe these Nb=O bonds to be the origin of strong acid sites on A-Nb_2O_5 for the following reasons: (i) both *n*-butylamine titration and pyridine adsorption showed stronger acid sites on A-Nb_2O_5 than P-Nb_2O_5, and only Nb=O bands are detected in the former, and (ii) the strongest acid sites disappear when A-Nb_2O_5 was heated to form TT-Nb_2O_5 and along with it, the loss of Raman features in the 850–1000 cm^{-1} region, which corresponds to NbO_6 octahedra containing Nb=O bonds. Furthermore, the enhancement in the acidity of A-Nb_2O_5 appears to come from Lewis acid sites. Recall that A-Nb_2O_5 has the same activity as P-Nb_2O_5 in the isomerization of 1-butene (see Table 5) which is catalyzed by Brønsted acid sites, and that pyridine preferentially desorbs from Brønsted acid sites upon evacuation (see Fig. 8). Finally, as A-Nb_2O_5 crystallizes into the T- and TT-forms after being heated at 873 and 1073 K, respectively, the loss in the strong acid sites is not accompanied by a loss in isomerization acidity. These results together suggest that A-Nb_2O_5 has strong Lewis acid sites but weak Brønsted acid sites.

In our previous work to relate the structure of niobia to acidity (*14*), we suggested that octahedral niobia, as one would find in crystalline Nb_2O_5, is mildly acidic, whereas tetrahedral niobia with a Nb=O bond is highly acidic. However, tetrahedral niobia can only be stabilized via oxide–oxide interactions, as in the cases of niobia on silica and niobia in silica (*14*). In the present study we showed that the preparation of an aerogel is in essence stabilizing NbO_6 octahedra with Nb=O bonds which have an intermediate acid strength. In terms of the heat of adsorption for pyridine, amorphous A-Nb_2O_5 has a value of ca. 30 kcal/mol, compared to ca. 20 kcal/mol for crystalline Nb_2O_5 and ca. 40 kcal/mol for tetrahedral niobia with a Nb=O bond (*14*). We re-

ported earlier a value of 32 kcal/mol for a silica-supported niobia containing a high concentration of niobia, for which a highly distorted octahedral structure with a Nb=O bond is also proposed. Our results thus demonstrate that sol–gel synthesis in conjunction with supercritical extraction is a viable way to stabilize a unique structure of bulk Nb_2O_5 with interesting acidic properties.

SUMMARY

We have successfully synthesized an aerogel of Nb_2O_5 which, after calcination at 773 K for 2 h, remains X-ray amorphous and has a BET surface area of 190 m^2/g. In order to achieve these characteristics, it is necessary to remove the solvent from the gel with supercritical CO_2, as conventional drying leads to a sample which is similar to precipitated Nb_2O_5.

Along with its high surface area, the amorphous Nb_2O_5 aerogel is more acidic than crystalline Nb_2O_5, as shown by *n*-butylamine titration and pyridine adsorption. The origin of acidity is ascribed to NbO_6 octahedra containing Nb=O bonds stabilized in a porous network, leading to strong Lewis acid sites.

These results show that the synthesis of aerogels is a promising avenue for preparing materials of catalytic interest. Work is underway in our laboratory to extend this approach to other single- and multi-component systems to understand the structure-acidity relationship in oxides.

ACKNOWLEDGMENTS

This work was supported in part by Niobium Products Company, Inc. One of us (S.M.M.) thanks the United States Army for a fellowship. We are grateful to Dr. J.-M. Jehng and Professor I. E. Wachs of Lehigh University for their help in performing the Raman experiments.

REFERENCES

1. Brinker, C. J., and Scherer, G. W., "Sol–Gel Science: The Physics and Chemistry of Sol–Gel Processing," Academic Press, New York, 1990.
2. Kistler, S. S., *Nature* **127,** 741 (1931).
3. Kistler, S. S., *J. Phys. Chem.* **36,** 52 (1932).
4. Ayen, R. J., and Iacobucci, P. A., *Rev. Chem. Eng.* **5,** 157 (1988).
5. Gesser, H. D., and Goswami, P. C., *Chem. Rev.* **89,** 765 (1989).
6. Kistler, S. S., Swann, S. Jr., and Appel, E. G., *Ind. Eng. Chem.* **26,** 388 (1934).
7. Teichner, S. J., Nicolanon, G. A., Vicarini, M. A., and Gardes, G. E. E., *Adv. Colloid Interface Sci.* **5,** 245 (1976).
8. Teichner, S. J., *in* "Aerogels, Proceedings of the First International Symposium" (J. Fricke, Ed.), p. 22. Springer-Verlag, Berlin, 1986.
9. Pajonk, G. M., *Appl. Catal.* **72,** 217 (1991).
10. Ko, E. I., and Maurer, S. M., *J. Chem. Soc., Chem. Commun.*, 1062 (1990).
11. Tanabe, K., *Catal. Today* **8,** 1 (1990).
12. Jehng, J.-M., and Wachs, I. E., *Catal. Today* **8,** 37 (1990).
13. Ko, E. I., Chen, J.-P., and Weissman, J. G., *J. Catal.* **105,** 511 (1987).
14. Burke, P. A., and Ko, E. I., *J. Catal.* **129,** 38 (1991).
15. Benesi, H. A., *J. Phys. Chem.* **61,** 970 (1957).
16. Deeba, M., and Hall, W. K., *Z. Phys. Chem.* **144,** 85 (1985).
17. Shafer, H., Gruehn, R., and Shulte, F., *Angew. Chem. Int. Ed. Engl.* **5,** 40 (1966).
18. Ko, E. I., and Weissman, J. G., *Catal. Today* **8,** 27 (1990).
19. Chen, Z., Iizuka, T., And Tanabe, K., *Chem. Lett.*, 1085 (1984).
20. Maurer, S. M., Ph.D. Thesis, Carnegie Mellon University, 1991.
21. Benesi, H. A., and Winquist, B. H. C., *Adv. Catal.* **27,** 97 (1978).
22. Basila, M. R., and Kantner, T., *J. Phys. Chem.* **70,** 1681 (1966).
23. Hightower, J. W., and Hall, W. K., *Am. Inst. Chem. Eng. Symp. Ser.* **63,** 122 (1967).
24. Goldwasser, J., Engelhardt, J., and Hall, W. K., *J. Catal.* **71,** 381 (1981).
25. Livage, J., Henry, M., and Sanchez, C., *Prog. Solid State Chem.* **18,** 259 (1988).
26. Alquier, C., Vandenborre, M. T., and Henry, M., *J. Non-Cryst. Solids* **79,** 383 (1986).
27. Vandenborre, M. T., Poumellec, B., Alquier, C., and Livage, J., *J. Non-Cryst. Solids,* **108,** 333 (1989).